Characterization of Buried Microstrip Lines for Constructing High-Density Microwave Integrated Circuits

Takahide Ishikawa and Eikichi Yamashita

Abstract—**This paper describes the characterization of a guided wave structure, buried microstrip line (BMSL), which is considered to be promising for constructing high-density microwave and millimeter-wave integrated circuits because of its high isolation characteristics. The BMSL includes a dielectric medium surrounded by ground conductor walls and a strip conductor on the top of the dielectric. The BMSL structure is characterized by the two methods, the rectangular boundary division (RBD) method and the finite-difference time-domain (FDTD) method. The RBD method is employed to obtain basic parameters of the BMSL such as characteristic impedances and coupling coefficients over a wide range of line sizes taking advantages of its high calculation efficiency. On the other hand, the FDTD method has been used for more detailed characterization such as the frequency performances of stub matching circuits. The FDTD method is also used to confirm the validity of the quasi-TEM wave approximation which the RBD is based on. The analysis results reveal that the BMSL structure possesses much lower coupling coefficients than a conventional microstrip line does, from −15 dB to −100 dB depending on their burial depths.**

I. Introduction

THERE HAVE been increasing demands for downsizing microwave and millimeter wave components including MIC's and MMIC's, because recent hand-carrying microwave apparatus such as personal mobile phones are required to be minimized in both weight and size. Despite such strong requirements, small sized or highly integrated microwave circuits have not been sufficiently developed. One of the reasons is that the high-density integration of MIC's and MMIC's forces us to make distances between interconnects in MIC's and MMIC's extremely short. Such short distances can lead to serious crosstalk between circuits, degradation in circuit performances, and even reliability problems. Several studies have been published in the past [1]–[2] on reducing coupling between two closely placed lines. However, guided wave structures with satisfactorily low coupling coefficients and applicability to MIC's or MMIC's have not been reported.

In this paper, we investigate buried microstrip line (BMSL) which possibly meets the above requirements. As shown in Fig. 1, a dielectric medium, through which electromagnetic waves propagate, is buried in a MIC's or MMIC's whose substrate is ceramic or semiconductor. A strip conductor is placed on the top of the buried dielectric, and ground conductor walls are formed to surround the buried dielectric. The BMSL can be incorporated into any types of supporting substrates including conductive materials, because electromagnetic waves are transmitted only in the buried dielectric which can be chosen arbitrarily regardless of the substrate. This feature enables us to fabricate silicon MMIC's easily. A similar structure has been studied as a single transmission line by Rozzi *et al.* [3]–[5]. To our knowledge, however, the crosstalk characterization of the structure for integrated circuits has not been reported.

The numerical analysis of the BMSL is conducted using the two types of calculation methods, the rectangular boundary division (RBD) method [6]–[8] and the finite-difference time-domain (FDTD) method [9]. The RBD method has been chosen to analyze basic transmission parameters such as characteristic impedance, coupling coefficients, and attenuation constants over a wide range of line dimensions taking advantages of its practicality and calculation efficiency. On the other hand, the FDTD has been utilized to obtain the isolation characteristics and the performances of short and open stub matching circuits. The FDTD method has been also used in part to confirm the validity of the quasi-TEM wave approximation of the RBD by comparing the coupling coefficients obtained from the RBD and those from the FDTD.

II. Basic Characterization of Buried Microstrip Lines with Rectangular Boundary Division Method

The RBD method is employed for the analysis, since the total region considered here can be easily divided into rectangular subregions suited to this simple and efficient method. This method is also suitable for calculating basic quasi-TEM wave parameters such as characteristic impedances, coupling coefficients, and attenuation constants over a wide range of the line dimensions because of its high calculation efficiency.

A. Analysis Procedures

The ground and strip conductors of the BMSL as shown in Fig. 2(a) are assumed to be lossless. Then an analytical model for the problem comes down to the one as shown in Fig. 2(b) consisting of the five regions. In this analysis, the thickness of the strip is assumed to be negligible. The potential in each

Manuscript received April 10, 1995; revised February 15, 1996.

T. Ishikawa is with the Optoelectronic and Microwave Devices Laboratory, Mitsubishi Electric Corporation 4-1 Mizuhara, Itami, Hyogo, 664 Japan.

E. Yamashita is with the Department of Electronic Engineering, University of Electro-Communications 1-5-1 Chofugaoka, Chofu-shi, Tokyo, 182 Japan.

Publisher Item Identifier S 0018-9480(96)03806-9.

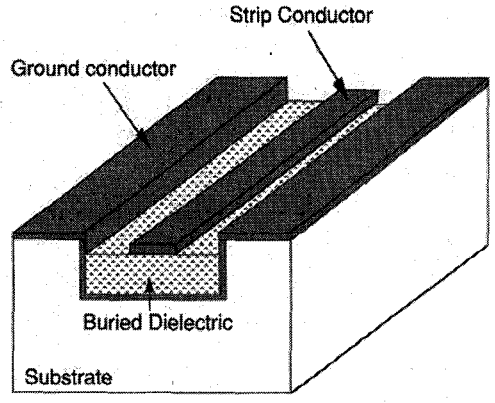

Fig. 1. Buried microstrip line (BMSL) which consists of a buried dielectric, a strip conductor, and a ground conductor surrounding the buried dielectric.

region can be expressed as

$$\phi_1 = \sum_{n=1}^{\infty} A_{1n} \sinh\{\xi_{1n}(y_1 - y)\} \sin\{\xi_{1n}(x - c_1)\} \quad \text{(region I)} \tag{1}$$

$$\phi_2 = \sum_{n=1}^{\infty} \{A_{2n} \sinh(\xi_{2n} y) + B_{2n} \cosh(\xi_{2n} y)\} \cdot \sin\{\xi_{2n}(x - c_2)\} \quad \text{(region II)} \tag{2}$$

$$\phi_3 = \sum_{n=1}^{\infty} A_{3n} \sinh\{\xi_{3n}(y - y_3)\} \sin\{\xi_{3n}(x - c_3)\} \quad \text{(region III)} \tag{3}$$

$$\phi_4 = \sum_{n=1}^{\infty} \{A_{4n} \sinh(\xi_{4n} y) + B_{4n} \cosh(\xi_{4n} y)\} \cdot \sin\{\xi_{4n}(x - c_4)\} \quad \text{(region IV)} \tag{4}$$

$$\phi_5 = \sum_{n=1}^{\infty} A_{5n} \sinh\{\xi_{5n}(y - y_5)\} \sin\{\xi_{5n}(x - c_5)\} \quad \text{(region V)} \tag{5}$$

where $\xi_{in} = n\pi/L_i$. (L is the length of each region and i is the region number.)

The Fourier series coefficients, $A_{1n}, A_{2n}, A_{3n}, A_{4n}, A_{5n}$, B_{2n}, and B_{4n}, are determined by minimizing the total electric field energy given by

$$U = \sum_{i=1}^{5} \frac{1}{2} \varepsilon_i \varepsilon_0 \iint \left[\left(\frac{\partial \phi_i}{\partial x} \right)^2 + \left(\frac{\partial \phi_i}{\partial y} \right)^2 \right] dx\, dy. \tag{6}$$

In order to simplify procedures for minimizing the total energy, we have adopted the first order spline function to express the boundary potentials as trial functions. For example, the first order spline function for the boundary potential $f(x)$ is expressed as

$$f(x) = \begin{cases} \dfrac{x - x_{j-1}}{x_j - x_{j-1}} p_j & x_{j-1} \le x \le x_j \\ \dfrac{x_{j+1} - x}{x_{j+1} - x_j} p_j & x_j \le x \le x_{j+1} \\ 0 & \text{elsewhere} \end{cases}. \tag{7}$$

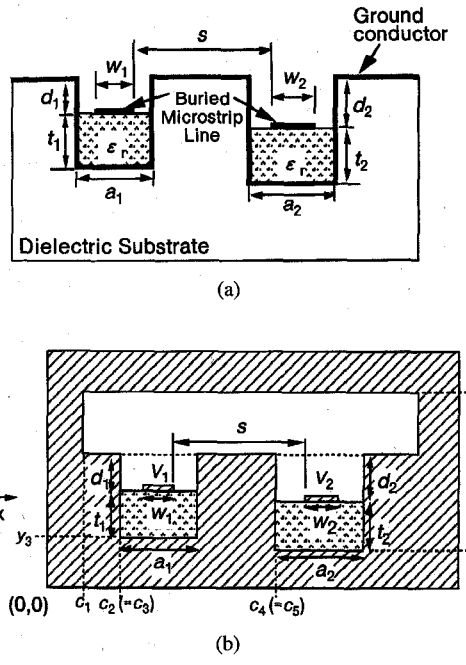

Fig. 2. (a) Cross-sectional view of the BMSL. (b) Analytical model consisting of five regions for applying the rectangular boundary division (RBD) method.

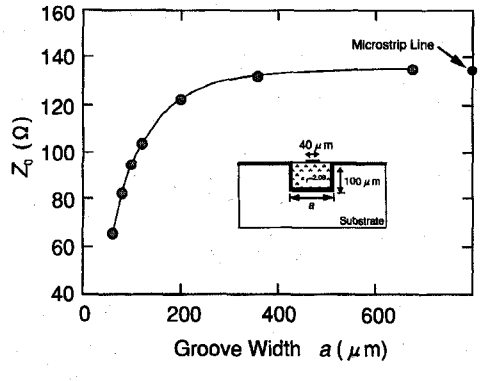

Fig. 3. Calculated characteristic impedance, Z_0, of BMSL as a function of groove width a when $t = 100\mu$m, $d = 0\mu$m, $w = 40\mu$m, and $\varepsilon_r = 2.08$. The Z_0 value increases when a is below 15 μm and then it tends to a constant value of about 135 ohms.

The total energy U is then minimized by taking a differentiation procedure as

$$\frac{\partial U}{\partial p_j} = 0 \qquad j = 2, 3, \cdots, m_1 - 1$$
$$\frac{\partial U}{\partial q_j} = 0 \qquad j = 2, 3, \cdots, m_2 - 1$$
$$\frac{\partial U}{\partial r_j} = 0 \qquad j = 2, 3, \cdots, m_3 - 1 \tag{8}$$

where m_1, m_2, and m_3 are the numbers of spline knot points, and p_j, q_j, and r_j are the potentials at the jth knot point of the spline functions for $f(x), g(x)$, and $h(x)$, respectively. When the p_j, q_j, and r_j are once calculated by minimizing the total energy, the value of C_{11} (the self capacitance of strip conductor 1), C_{12} ($= C_{21}$ the mutual capacitance between the conductors 1 and 2), and C_{22} (the self capacitance of the strip

conductor 2) are readily calculated by

$$C_{11} = 2U_{\min}(1) \tag{9}$$

$$C_{22} = 2U_{\min}(2) \tag{10}$$

$$C_{12} = U_{\min}(3) - U_{\min}(1) - U_{\min}(2) \tag{11}$$

where $U_{\min}(1), U_{\min}(2)$, and $U_{\min}(3)$ are the minimum energy values for the case 1 ($V_1 = 1$ V, $V_2 = 0$ V), the case 2 ($V_1 = 0$ V, $V_2 = 1$ V), and the case 3 ($V_1 = V_2 = 1$ V), respectively. Then the characteristic impedances for the even and odd modes are obtained by applying

$$Z_M = \frac{1}{v_0\sqrt{C_M C_{0M}}} \quad M = \text{even or odd} \tag{12}$$

where

$$C_{\text{even}} = C_{11} + C_{12} \tag{13}$$

$$C_{\text{odd}} = C_{11} - C_{12} \tag{14}$$

$$C_{0\text{even}} = C_{011} + C_{012} \tag{15}$$

$$C_{0\text{odd}} = C_{011} - C_{012} \tag{16}$$

v_0 = light velocity in vacuum.

C_{011}, C_{012}, and C_{022} are the capacitance values of C_{11}, C_{12}, and C_{22} for the case where all the dielectric constants are replaced by ε_0.

B. Numerical Results

1) Characteristic Impedance: The characteristic impedance of the BMSL has been calculated for the model of Fig. 2(b) with a sufficiently large distance between the two BMSL's s so that the coupling between them can be neglected. Fig. 3 shows the calculated characteristic impedance Z_0 of the BMSL compared with that of the microstrip line of the same dielectric thickness, the same dielectric constant, and the same strip conductor width as a function of the groove width a when $t = 100$ μm, $d = 0$ μm, $w = 40$ μm, and $\varepsilon_r = 2.08$. The characteristic impedance of the microstrip line has been also obtained by the RBD method. As seen in the figure, Z_0 increases with the increase of a when a is below about 15 μm and for over 15 μm it becomes saturated to a constant value of 135 ohms. The increase and saturation of Z_0 is explained as follows. The capacitance C_{11} (or C_{22}) and C_{011} (or C_{022}) decrease as a increases and the capacitance decrease leads to the Z_0 decrease. When a becomes larger the groove wall effect can be neglected in terms of the electromagnetic fields analysis, consequently the transmission line behaves as a microstrip line.

2) Coupling Characteristics: The coupling coefficients of the two parallel BMSL's and of microstrip lines are calculated in order to investigate the crosstalk characteristics of the BMSL's. The coupling coefficient k is defined as usual as follows

$$k = \frac{Z_{\text{even}} - Z_{\text{odd}}}{Z_{\text{even}} + Z_{\text{odd}}} \tag{17}$$

where Z_{even} and Z_{odd} are determined as

$$Z_M = \frac{1}{v_0\sqrt{C_M C_{0M}}}. \tag{18}$$

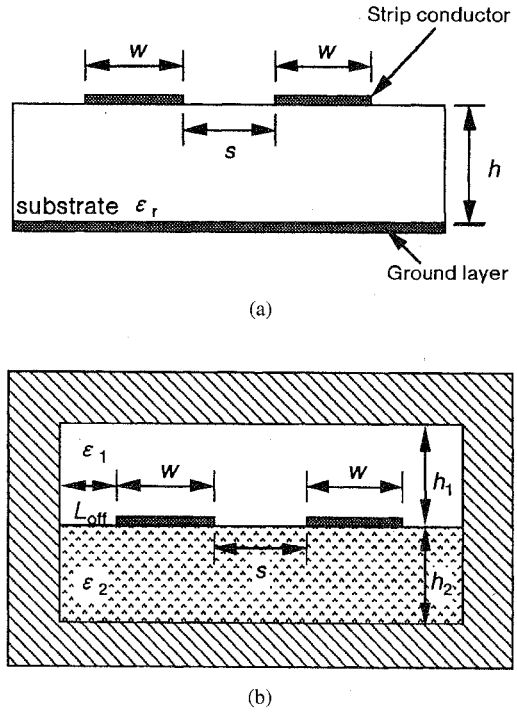

Fig. 4. (a) Cross-sectional view of parallel microstrip lines. (b) Analytical model for obtaining the coupling coefficients of the microstrip lines by the RBD method.

(v_0 = light velocity in vacuum, C_M = capacitance with dielectric, C_{M0} = capacitance without dielectric, M =mode designation (even or odd).)

Fig. 4(a) and (b) show the cross-sectional view and the analytical model for the calculation of the coupling coefficients of microstrip lines, respectively. Fig. 5(a) and (b) show the calculated coupling coefficients k of the BMSL's as a function of a distance between the two lines s for comparison with the k values of microstrip lines with the same dielectric thickness, dielectric constant, and strip conductor width. The results shown in Fig. 5(a) are for $a_1 = a_2 = 150$ μm, $t_1 = t_2 = 100$ μm, $d_1 = d_2 = 0, 50, 100, 150$ μm, $w_1 = w_2 = 50$ μm, and $\varepsilon_r = 3.4$. Those shown in Fig. 5(b) are for $a_1 = a_2 = 100$ μm, $t_1 = t_2 = 100$ μm, $d_1 = d_2 = 0, 50, 100, 150$ μm, $w_1 = w_2 = 50$ μm, and $\varepsilon_r = 3.4$. As seen in these figures, the BMSL possesses extremely low coupling coefficients compared with conventional microstrip lines, especially with the increase of burial depth d. In Fig. 5(a) BMSL has about 20 dB lower coupling coefficients than microstrip lines have when $d = 0$ μm. The k value decreases about 20 dB for each increment for every 50 μm increase of d. In Fig. 5(b) the BMSL has about 30 dB lower k values than microstrip lines have at $d = 0$ μm, and k decrease about 30 dB for each 50 μm increment of d. Comparison of Fig. 5(a) with Fig. 5(b) also discloses that the coupling coefficients become much smaller when the width of the buried dielectric becomes narrower because of the stronger containment effect of propagating waves. When the dimensions are chosen to be $a_1 = a_2 = 100$ μm and $d_1 = d_2 = 150$ μm, the k values of BMSL become extremely low values as -100 dB.

The candidates of buried dielectric material can be polyimide or SiO_2 because these have been usually employed as

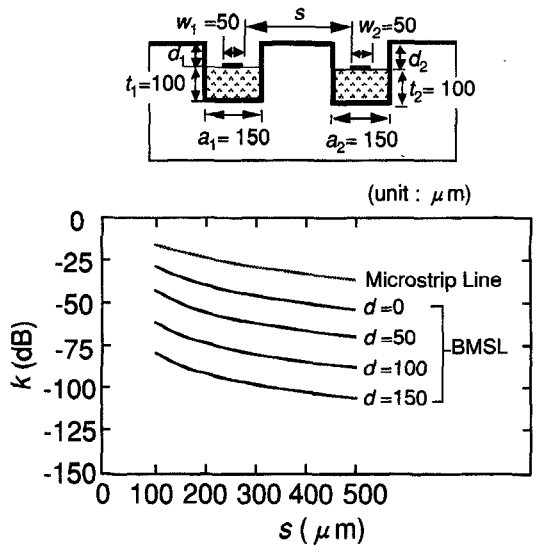

(a)

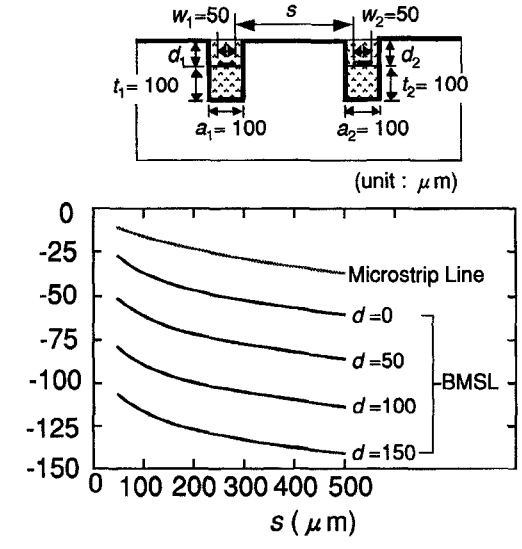

(b)

Fig. 5. Calculated coupling coefficients, k, of BMSL's as a function of the distance between the two lines, s, for comparison with the k values of microstrip lines with the same dielectric thickness, dielectric constant, and strip conductor width. (a) Results for $a_1 = a_2 = 150\ \mu\text{m}, t_1 = t_2 = 100\ \mu\text{m}, d_1 = d_2 = 0, 50, 100, 150\ \mu\text{m}, w_1 = w_2 = 50\ \mu\text{m}$, and $\varepsilon_r = 3.4$. (b) Results for $a_1 = a_2 = 100\ \mu\text{m}, t_1 = t_2 = 100\ \mu\text{m}, d_1 = d_2 = 0, 50, 100, 150\ \mu\text{m}, w_1 = w_2 = 50\ \mu\text{m}$, and $\varepsilon_r = 3.4$.

isolation materials of interconnects or passivation layers in MMIC's and their reliability has already been confirmed. From these results, we conclude that the BMSL structure should be useful in constructing highly isolated transmission lines for realizing high-density microwave integrated circuits.

3) Attenuation Constant: In this section the attenuation constant of BMSL's are calculated for different groove width a using the RBD method. The symmetry of the structure is considered in the model as shown in Fig. 6, which also includes the finite strip conductor thickness so that the capacitance difference formula [8] can be applied. The formula is

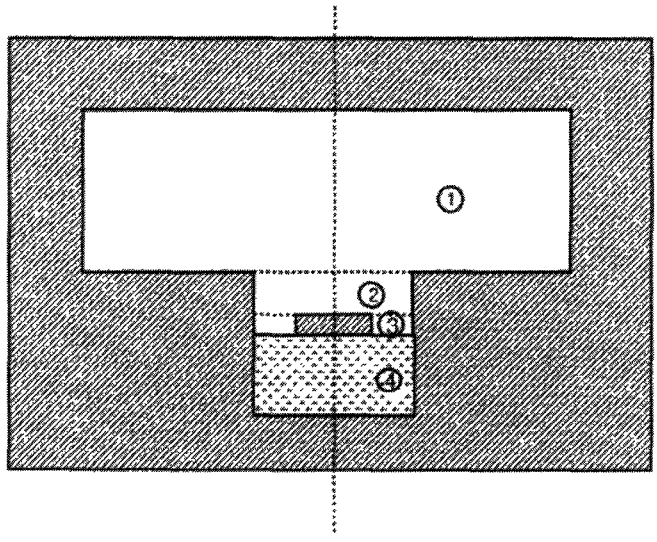

Fig. 6. Analysis model consisting of four regions with the consideration of symmetry for loss analysis.

$$\alpha_c = \frac{\pi}{\lambda}\left(\frac{C_0}{C_0'} - 1\right) \tag{19}$$

where α_c is the attenuation constant caused by the conductor loss of the BMSL, λ is the wave length of the propagating wave, C_0 is the capacitance of the strip conductor for the case where the dielectric constant of all the dielectric layers are ε_0. C_0' is the capacitance of the strip conductor when the all conductor surfaces are recessed by $\delta_s/2$, where δ_s is the skin depth of the conductor given by

$$\delta_s = \sqrt{\frac{2\rho}{\omega\mu_0}} \tag{20}$$

where μ_0 is the permeability, and ρ is the resistivity of the conductor. Before the calculation of the attenuation constant, the characteristic impedance is calculated for the same dimensions (except for the conductor thickness 5 μm employed in Fig. 2(b) and compared with each other in order to confirm the validity of the RBD method. The numerical results for each model have shown excellent agreement within 1 percent difference, therefore, they indicate that both analytical models are reasonable. Fig. 7 shows the calculation results as a function of the frequency for the case of $t_1 = t_2 = 2\ \text{mm}, d_1 = d_2 = 0\ \text{mm}, w_1 = w_2 = 1\ \text{mm}, \varepsilon_r = 3.4$, and the conductor thickness is 5 μm. This figure shows that when the groove width a becomes larger the attenuation constant decreases accordingly.

III. Detailed Characterization of Buried Microstrip Lies with Finite-Difference Time-Domain Method

In the previous section, various numerical results based on the quasi-TEM wave approximation have been obtained with the use of the RBD method. In this section, the more detailed characterization based on the fullwave analysis with the FDTD [9] is conducted to calculate the coupling coefficients and the characteristics of the stub matching circuits with the BMSL's. The reason for using the FDTD is that the method is quite suitable for analyzing the problems with structure discontinuity

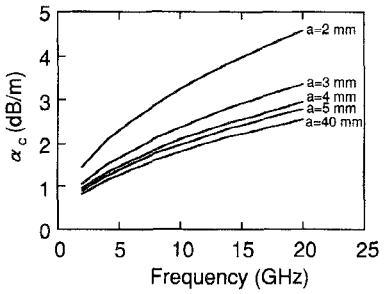

Fig. 7 Conductor loss as a function of frequency for the case where $t_1 = t_2 = 2$ mm, $d_1 = d_2 = 0$ mm, $w_1 = w_2 = 1$ mm, $\varepsilon_r = 3.4$, and the conductor thickness is 5 μm. This figure shows that when the groove width a becomes large the loss decreases accordingly

such as stub matching circuits treated in this part, on the ground that it automatically takes into consideration the effect of the material and structural discontinuity of the model although the FDTD method usually needs a super computer and a long calculation time. Also the validity of the quasi-TEM wave approximation with less computation cost is confirmed by comparing the results with the FDTD method and with the RBD method.

A. Analysis Procedures

Formulation of the FDTD method begins with Maxwell's curl equations. For simplicity, the media are assumed to be piecewise uniform, isotropic, and homogeneous. The structure is assumed to be lossless. Maxwell's curl equations are written as

$$\nabla \times E = -\mu \frac{\partial H}{\partial t} \tag{21}$$

$$\nabla \times H = \sigma E + \varepsilon \frac{\partial E}{\partial t}. \tag{22}$$

In order to find an approximate solution to this set of equations, the region to be analyzed is discretized with finite three-dimensional computational cells with appropriate boundary conditions enforced on the source, conductors, and cell walls.

B. Numerical Results

1) Coupling Characteristics: The objective of this part of research is to investigate more on the coupling characteristics versus frequency using the fullwave analysis of the FDTD. The analytical model adopted here is shown in Fig. 8(a) and (b) which contains two parallel-coupled BMSL's (l = 17.5 mm) and four termination resistors with the resistance value matched to the characteristic impedance of the lines. This method has been reported in the literature [10] which showed that reflected coefficients at the termination were less than 0.1 at frequencies under 10 GHz. The setting of the resistance is conducted by applying a finite conductivity value of σ in (22), while for other portion of the model σ is set as zero. The value of σ is defined as

$$\sigma = \frac{1}{R} \frac{\Delta x \cdot n_x}{\Delta y \cdot n_y \cdot \Delta z \cdot n_z}. \tag{23}$$

The input signal to Port 1 is a Gaussian pulse whose waveform is given by

$$E_x(t\Delta t) = \exp\left(-\frac{(t-t_0)^2}{T^2}\right). \tag{24}$$

The values of t_0 and T are set as 270 and 90 time steps, respectively, which gives the maximum analysis frequency of 20 GHz. The cell size is set as $\Delta x = 0.5$ mm, $\Delta y = 0.25$ mm, and $\Delta z = 0.25$ mm. The time step is $\Delta t = 0.4$ ps, which are derived from the Courant condition [11] given as

$$v\Delta t \leq \frac{1}{\sqrt{\frac{1}{(\Delta x)^2} + \frac{1}{(\Delta y)^2} + \frac{1}{(\Delta z)^2}}}. \tag{25}$$

The adopted absorbing boundary conditions are Mur's first and second order conditions [12]. The numbers of the cells are $n_x = 30, n_y = 48$, and $n_z = 130$. The calculation has been carried out on a Hewlett Packard workstation and the CPU time consumed in the calculation was 4510 seconds for this case. To compare the isolation characteristics analyzed by the RBD with those by the FDTD, s-parameters are computed based on the quasi-TEM parameters using a method introduced by Yamamoto *et al.* [13]. The detailed procedures are shown in Appendix. This method is especially adequate for crosstalk analysis because it can provide output signals for the isolation port, while traditional methods do not [14]. Fig. 9(a) and (b) show examples of the calculated s-parameters for the case of $a_1 = a_2 = 2mm, t_1 = t_2 = 2mm, d_1 = d_2 = 3mm, w_1 = w_2 = 1mm, s = 1.5mm$, and $\varepsilon_r = 3.4$ to compare the results with the RBD method and with the FDTD method. Fig. 9(a) shows the s-parameters for the isolation port (Port 3), and Fig. 9(b) shows those for the coupling port (Port 4). These figures clearly demonstrate a good agreement of the numerical results based on the RBD and those on the FDTD. This fact verifies that the quasi-TEM mode assumption is valid and the isolation characteristics calculated by the RBD shown earlier are sufficiently accurate for the BMSL structure of the present dimensions. The obtained results are very significant because when BMSL's are incorporated in MIC's and MMIC's, the design of BMSL circuits can be substantially simplified by using the quasi-TEM approximation. It is also clarified from the analyses that the FDTD method is convenient to handle such low signal power levels, which corresponds to a calculation dynamic range as much as 140 dB.

2) Characteristics of Stub Matching Circuits: In order to use BMSL for MIC's and MMIC's, the matching circuits are also required to construct practical microwave and millimeter-wave circuits. In this part, the feasibility of short and open stubs of the BMSL's are investigated by analyzing their frequency characteristics using the FDTD method. The model employed for the computation is as shown in Fig. 10(a) and (b). The stub length is set as 37.5 mm, The dielectric and discretized parameters are the same as in Fig. 8. The cell sizes are $n_x = 12, n_y = 200$, and $n_z = 88$. The numerical results are shown in Fig. 11(a) and (b) for the short and open stubs, respectively. The transmission frequencies are obtained with the quasi-TEM approximation by calculating the following

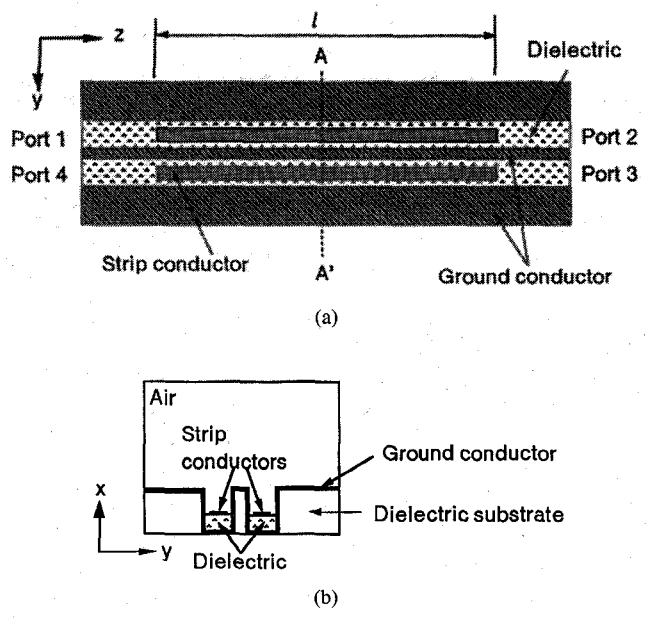

Fig. 8. Analytical model adopted for calculating the crosstalk of BMSL's by FDTD. The model contains two parallel-coupled BMSL's ($l = 17.5$ mm) and four termination resistors with the resistance value matched to the characteristic impedance of the lines. (a) Top view of the model, and (b) cross-sectional view of the model.

formula

$$\lambda = \frac{\nu_0}{f} \Big/ \sqrt{\varepsilon_{\text{eff}}}. \tag{26}$$

In (26), the value of ε_{eff} has been already determined as $\varepsilon_{\text{eff}} = 2.33$ by the RBD method. The transmitting frequency f_{ts} for the short stub is given as

$$f_{ts} = 1.31 \times (2n-1) \quad (\text{GHz}) \qquad n = 1, 2, 3, \cdots \tag{27}$$

and the shunt frequency f_{ss} for short stub is

$$f_{ss} - 1.31 \times 2n \quad (\text{GHz}) \qquad n = 1, 2, 3, \cdots \tag{28}$$

and transmitting frequency f_{to} for open stub is

$$f_{to} = 1.31 \times 2n \quad (\text{GHz}) \qquad n = 1, 2, 3, \cdots \tag{29}$$

and shunt frequency f_{so} for open stub is

$$f_{so} = 1.31 \times (2n-1) \quad (\text{GHz}) \qquad n = 1, 2, 3, \cdots. \tag{30}$$

In Fig. 11(a) and (b), these formula show fairly good agreements with the results from FDTD method, showing that stub matching circuits such as short and open stubs are available for BMSL circuits in the same way as in MIC's and MMIC's using microstrip lines. These results clearly indicate that the MIC's and MMIC's using BMSL's are readily realized by using short and open stub circuits as microstrip circuits. This fact enhances very much the versatility of the BMSL.

IV. Conclusion

The BMSL structure was proposed for constructing high-density microwave integrated circuits. A variety of characteristics of the BMSL were analyzed and compared with those of conventional microstrip lines by using the RBD and the FDTD methods. It has been revealed that the structure possesses extremely low coupling coefficients compared with those of microstrip lines from -15 to -100 dB for the above dimensions. The FDTD analyses verified the validity of the quasi-TEM assumption for the structure of the present dimensions, showing that the basic design of MIC's and MMIC's of BMSL's is quite simple by using the quasi-TEM parameters. The stub matching circuits of the BMSL's can be realized in the same way as microstrip circuits. The BMSL is expected to be utilized in high-density MIC's and MMIC's for its low cross-talk characteristics.

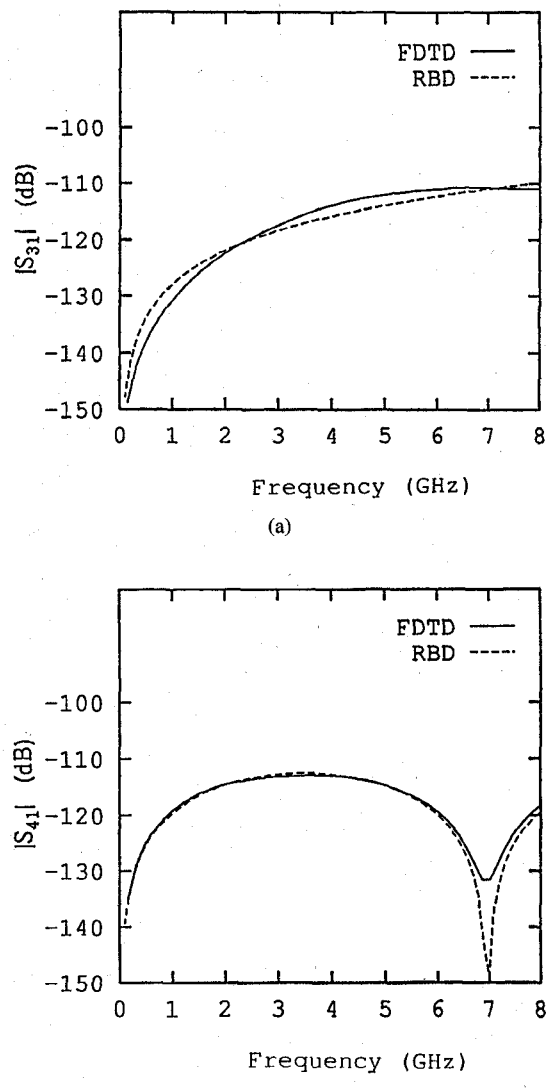

Fig. 9. Calculated s-parameters for the case of $a_1 = a_2 = 2$ mm, $t_1 = t_2 = 2$ mm, $d_1 = d_2 = 3$ mm, $w_1 = w_2 = 1$ mm, $s = 1.5$mm, and $\varepsilon_r = 3.4$ to compare the results with the RBD method and with the FDTD method. (a) S-parameters for the isolation port (Port 3). (b) S-parameters for the coupling port (Port 4).

Appendix

In the method, electric or magnetic fields for each port are obtained as

$$c_1 = (\Gamma_e + \Gamma_0)/2 \tag{31}$$

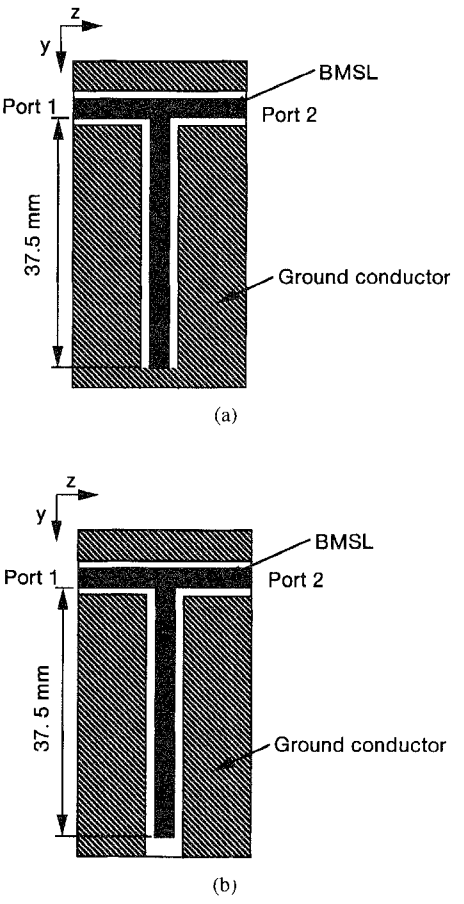

Fig. 10. Models employed for the calculation of the characteristics of short and open stubs of the BMSL's with the use of the FDTD method The stub length is set as 37.5 mm. The dielectric and discretized parameters are the same as in Fig. 4 (a) Short stub. (b) Open stub.

$$c_2 = (\Gamma_e + \Gamma_0)/2 \tag{32}$$

$$c_3 = (\Gamma_e + \Gamma_0)/2 \tag{33}$$

$$c_4 = (\Gamma_e - \Gamma_0)/2 \tag{34}$$

where $c_1 - c_4$ are electric or magnetic fields for each port (Port 1, 2, 3, and 4), and T_e, T_o, Γ_e, and Γ_o are a transmission coefficient for the even mode, a transmission coefficient for the odd mode, a reflection coefficient for the even mode, and a reflection coefficient for the odd mode, respectively. These reflection and transmission coefficients are defined as

$$\Gamma_e = \frac{A_e + B_e - C_e - D_e}{A_e + B_e + C_e + D_e} \tag{35}$$

$$\Gamma_0 = \frac{A_0 + B_0 - C_0 - D_0}{A_0 + B_0 + C_0 + D_0} \tag{36}$$

$$T_0 = \frac{2}{A_0 + B_0 + C_0 + D_0} \tag{37}$$

$$T_e = \frac{2}{A_e + B_e + C_e + D_e} \tag{38}$$

where $A_e, A_o, B_e, B_o, C_e, C_o, D_e$, and D_o are given by

$$A_e = \cos(\beta_e l) \tag{39}$$

$$A_0 = \cos(\beta_0 l) \tag{40}$$

$$B_e = jZ_e \sin(\beta_e l) \tag{41}$$

$$B_0 = jZ_0 \sin(\beta_0 l) \tag{42}$$

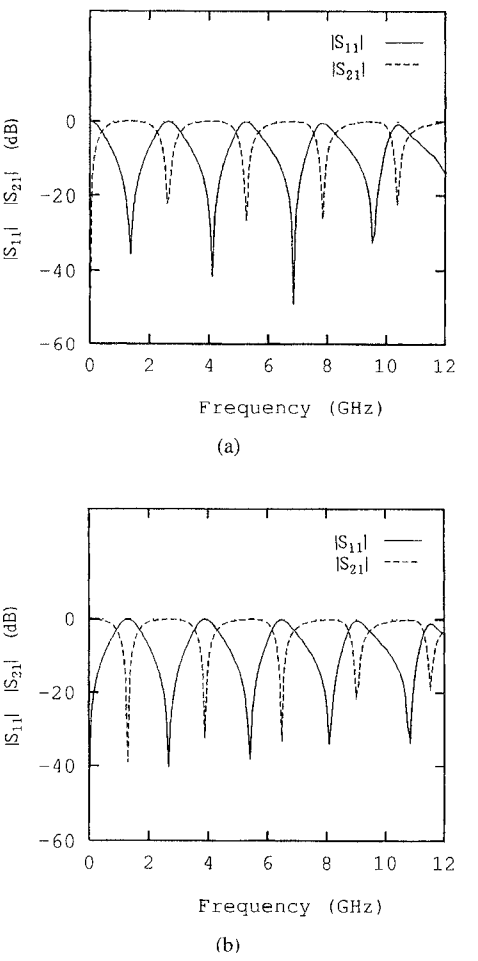

Fig. 11. Numerical results of the stubs as a function of frequency. The results show good agreement with those by the quasi-TEM approximation. (a) Results for short stub. (b) Results for open stub.

$$C_e = j\frac{1}{Z_e}\sin(\beta_e l) \tag{43}$$

$$C_0 = j\frac{1}{Z_0}\sin(\beta_0 l) \tag{44}$$

$$D_e = \cos(\beta_e l) \tag{45}$$

$$D_0 = \cos(\beta_0 l) \tag{46}$$

where β_e and β_o are the phase constants for the even mode and for the odd mode, respectively. l is the coupling length.

ACKNOWLEDGMENT

The authors would like to thank Dr. N. Kishi and Dr. Y. Qian for their useful discussion through this work. They also gratefully acknowledge Dr. O. Ishihara, N. Tanino, H. Takano, and H. Oohashi of Mitsubishi Electronic Corporation for their continuous support for the study.

REFERENCES

[1] S. He, A. Z. Elsherbeni, and C. Smith, "Decoupling between two conductor microstrip transmission line," *IEEE Trans. Microwave Theory Tech.*, vol. 41, no. 1, pp. 53–61, Jan. 1993.

[2] N. G. Alexopoulos and C. M. Krowne, "Characteristics of single and coupled microstrips on anisotropic substrates," *IEEE Trans. Microwave Theory Tech.*, vol. 26, no. 6, pp. 387–393, June 1978.

[3] T. Rozzi, A. Morini, and G. Gerini, "Analysis and applications of microstrip-loaded inset dielectric waveguide (MIG)," *IEEE Trans. Microwave Theory Tech.*, vol. 40, no. 2, pp. 272–278, Feb. 1992.
[4] N. Izzat, S. R. Pennock, and T. Rozzi, "Space domain analysis of micro-IDG structures," *IEEE Trans. Microwave Theory Tech.*, vol. 42, no. 6, pp. 1074–1078, June 1994.
[5] T. Rozzi, G. Gerini, A. Morini, and M. De Santis, "Multilayer buried microstrip inset guide," in *European Microwave Conf. Dig.*, 1991, pp. 673–678.
[6] E. Yamashita, Masayuki Nakajima, and Kazuhiko Atsuki, "Analysis method for generalized suspended striplines," *IEEE Trans. Microwave Theory Tech.*, vol. MTT-34, no. 12, pp. 1457–1463, Dec. 1986.
[7] H. Takasu, and E. Yamashita, "Impedance characterization of GaAs FET switches," *IEEE Trans. Microwave Theory Tech.*, vol. 40, no. 7, pp. 1422–1429, July 1992.
[8] E. Yamashita, K. R. Li, and Y. Suzuki, "Characterization method and simple design formulas of MCS lines proposed for MMIC's," *IEEE Trans. Microwave Theory Tech.*, vol. MTT-35, no. 12, pp. 1355–1362, Dec. 1987.
[9] K. S. Yee, "Numerical solution of initial boundary value problems involving Maxwell's equations in isotropic media," *IEEE Trans. Antennas Propagat.*, vol. AP-14, pp. 302–307, May 1966.
[10] M. Piket-May, A. Taflove, and J. Baron, "FD-TD modeling of digital signal propagation in 3-D circuits with passive and active loads," *IEEE Trans. Microwave Theory Tech.*, vol. 42, no. 8, pp. 1514–1523, Aug. 1994.
[11] A. Taflove, and M. E. Brodwin, "Numerical solution of steady-state electromagnetic scattering problems using the time-dependent Maxwell's equations," *IEEE Trans. Microwave Theory Tech.*, vol. MTT-23, pp. 623–630, 1975.
[12] G. Mur, "Absorbing boundary condition for the finite-difference approximation of the time-domain electromagnetic-field equations," *IEEE Trans. Electromag. Compat.*, vol. EC-23, no. 4, pp. 377–382, 1981.
[13] S. Yamamoto, T. Azakami, and K. Itakura, "Coupled nonuniform transmission line and its applications," *IEEE Trans. Microwave Theory Tech.*, vol. MTT-15, no. 4, pp. 220–231, Apr. 1967.
[14] T. Edwards, *Foundations for Microstrip Circuit Design*, 2nd ed. New York: Wiley, 1992.

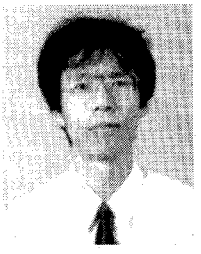

Takahide Ishikawa was born in Kagawa, Japan, on July 2, 1958. He received the B.S. and M.S. degrees in electronic engineering from the University of Electro-Communications, Tokyo, Japan, in 1981 and 1983, respectively.

In 1983 he joined the LSI Research and Development Laboratory, Mitsubishi Electric Corporation, Hyogo, Japan. Since then he has been engaged in the development of GaAs MMIC process and device technologies especially in FET amplifiers for low-noise and high power applications. He is currently an Assistant Manager in the GaAs IC Engineering Group, Microwave Devices Development Department, Optoelectronic and Microwave Devices Laboratory, Hyogo, Japan. He also is a student in the doctoral course of the University of Electro-Communications, Tokyo, Japan. His research interests include numerical analyzes and experiments on microwave and millimeter-wave circuits.

Mr. Ishikawa is a member of the Institute of Electronics, Information, and Communication Engineers of Japan.

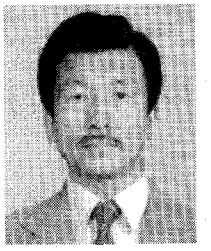

Eikichi Yamashita was born in Tokyo, Japan, on February 4, 1933. He received the B.S. degree from the University of Electro-Communications, Tokyo, Japan, and the M.S. and Ph.D. degrees from the University of Illinois, Urbana, IL, all in electrical engineering, in 1956, 1963, and 1966, respectively.

From 1956 to 1964, he was a Member of the research staff on millimeter-wave engineering at the Electrotechnical Laboratory, Tokyo, Japan. While on leave from 1961 to 1963 and from 1964 to 1966, he studied solid-state devices in the millimeter-wave region at the the Electro-Physics Laboratory, University of Illinois. He became Associate Professor in 1967 and Professor in 1977 in the Department of Electronic Engineering, Dean of Graduate School from 1992 to 1994, the University of Electro-Communications, Tokyo, Japan. His research work since 1956 has been principally on applications of electromagnetic waves such as various microstrip transmission lines, wave propagation in gaseous plasma, pyroelectric-effect detectors in the submillimeter-wave region, tunnel-diode oscillators, wide-band laser modulators, various types of optical fibers, ultra-short electrical pulse propagation on transmission lines, and millimeter-wave imaging. He edited the book, *Analysis Methods for Electromagnetic Wave Problems (vol. 1 and vol. 2)*, (Norwood, MA: Artech House).

Dr. Yamashita was Chairperson of the Technical Group on Microwaves, IEICE, Japan, for the period 1985 to 1986, and Vice-Chairperson, Steering Committee, Electronics Group, IEICE, for the period 1989 to 1990. He is a Fellow of IEEE, and served as Associate Editor of the IEEE TRANSACTIONS ON MICROWAVE THEORY AND TECHNIQUES during the period 1980 to 1984. He was elected Chairperson of the MTT-S Tokyo Chapter for the period 1985 to 1986. He has been a member of the MTT-S ADCOM since January 1992, and Chairperson of Chapter Operations Committee, IEEE Tokyo Section, since 1995. He served as Chairperson of International Steering Committee, 1990 and 1994 Asia-Pacific Microwave Conference, held in Tokyo and sponsored by the IEICE.